

Original Paper

*Both authors contributed equally to this work and share first authorship credit.

Cite this article: Logar-Henderson C, Ling R, Tuite AR, Fisman DN (2019). Effects of large-scale oceanic phenomena on non-cholera vibriosis incidence in the United States: implications for climate change. *Epidemiology and Infection* **147**, e243, 1–7. <https://doi.org/10.1017/S0950268819001316>

Received: 18 April 2019

Revised: 7 June 2019

Accepted: 13 June 2019


Key words:

Climate change; foodborne illness; *Vibrio fluvialis*; *Vibrio parahaemolyticus*; *Vibrio vulnificus*

Author for correspondence:

David N. Fisman, E-mail: david.fisman@utoronto.ca

Effects of large-scale oceanic phenomena on non-cholera vibriosis incidence in the United States: implications for climate change

Chloë Logar-Henderson^{1,*}, Rebecca Ling^{1,*}, Ashleigh R. Tuite¹ and David N. Fisman^{1,2} 

¹Dalla Lana School of Public Health, University of Toronto, Toronto, Ontario, Canada and ²Division of Infectious Diseases, Department of Medicine, Faculty of Medicine, University of Toronto, Toronto, Ontario, Canada

Abstract

Non-cholera *Vibrio* (NCV) species are important causes of disease. These pathogens are thermophilic and climate change could increase the risk of NCV infection. The El Niño Southern Oscillation (ENSO) is a ‘natural experiment’ that may presage ocean warming effects on disease incidence. In order to evaluate possible climatic contributions to observed increases in NCV infection, we obtained NCV case counts for the United States from publicly available surveillance data. Trends and impacts of large-scale oceanic phenomena, including ENSO, were evaluated using negative binomial and distributed non-linear lag models (DNLM). Associations between latitude and changing risk were evaluated with meta-regression. Trend models demonstrated expected seasonality ($P < 0.001$) and a 7% (6.1%–8.1%) annual increase in incidence from 1999 to 2014. DNLM demonstrated increased vibriosis risk following ENSO conditions over the subsequent 12 months (relative risk 1.940, 95% confidence interval (CI) 1.298–2.901). The ‘relative–relative risk’ (RRR) of annual disease incidence increased with latitude (RRR per 10° increase 1.066, 95% CI 1.027–1.107). We conclude that NCV risk in the United States is impacted by ocean warming, which is likely to intensify with climate change, increasing NCV risk in vulnerable populations.

Introduction

Bacteria of the genus *Vibrio* are found in surface waters in the Americas, Asia, Europe and Australia and are responsible for causing several types of human infections, including cholera and non-cholera vibriosis (NCV) [1, 2]. While cholera is typically caused by toxigenic *Vibrio cholerae* serogroups O1 or O139, vibriosis is caused by non-toxicogenic *V. cholerae* serogroups and roughly 12 other *Vibrio* species including *V. vulnificus*, *V. parahaemolyticus* and *V. fluvialis* [3, 4]. While most individuals with vibriosis develop symptoms such as diarrhoea and abdominal pain, some (particularly those with liver disease or immune compromise) may experience skin and soft tissue infection (typically characterised by bullous skin lesions) and septic shock [5]. Infection can be transmitted by food or by exposure to contaminated salt-water, and the most severely affected individuals often have immune compromise or liver disease [5]. Infections display summertime seasonality, which is believed to reflect the thermophilic nature of these bacteria, as well as increased leisure-related salt-water exposure and harvesting of seafood in the summer [1].

There has been an increase in NCV reported in recent decades in the United States [3]. In 1988, the US Centers for Disease Control and Prevention (CDC) established the Cholera and Other *Vibrio* Illness Surveillance (COVIS) system, which initially focused on states (Texas, Alabama and Louisiana) forming part of the Gulf of Mexico coastline and expanded through the 1990s. By 2007, it was established as a national surveillance system at which time NCV became nationally notifiable [3, 6]. The system relies on reports of laboratory-confirmed vibriosis cases from state and territorial public health authorities [3, 6]. The reason for increased incidence of NCV in the United States is unclear, but might reflect improved case ascertainment, emergence of novel vibrio strains [7] or increased abundance of the pathogen due to increasing ocean temperatures. Recent, concurrent, increases in NCV in the Baltic region of Europe appear to be linked to warming Baltic Sea-surface temperatures and may be a result of anthropogenic climate change [8].

Large-scale climatic phenomena may provide an important natural experiment that improves understanding of the potential future impacts of climate change on infectious disease risk. For example, the impact of the El Niño Southern Oscillation (ENSO) on cholera risk has been well-studied [9, 10]. The irregular and periodic nature of ENSO, and the similarity of ENSO-linked weather anomalies to those projected to occur with greater frequency with climate change, make ENSO a powerful natural experimental system for understanding the

© The Author(s) 2019. This is an Open Access article, distributed under the terms of the Creative Commons Attribution licence (<http://creativecommons.org/licenses/by/4.0/>), which permits unrestricted re-use, distribution, and reproduction in any medium, provided the original work is properly cited.

potential impact of climate change on infectious diseases and other health and economic issues [11]. Oceanic warming and extreme weather events including heat waves and hurricanes have also been associated with range expansion for vibriosis risk [12] and NCV outbreaks, respectively [13]. To our knowledge, the impact of ENSO and other large-scale climatic phenomena on vibriosis risk in the United States has not been previously examined.

We combined environmental exposure data with national and state-level vibriosis case counts derived from the COVIS system to evaluate the degree to which variation in vibriosis risk in the United States and in U.S. regions might be explained by large-scale climatic phenomena such as ENSO. We also performed exploratory regional analyses to evaluate regional differences in evolving vibriosis risk, and to evaluate the possibility that changing patterns of risk are consistent with vibriosis range expansion.

Methods

Non-cholera vibriosis data

Annual COVIS reports containing vibriosis case counts in the United States from 1997 to 2014 are publicly available, and were obtained from the United States Centre for Disease Control and Prevention [14]. The initial report, which included aggregate data for 1997 and 1998, was not used. Annual reported vibriosis case counts, by state, were extracted manually from published maps. Monthly national case counts were available from published graphs; we used the WebPlotDigitizer application (version 4.1) to accurately estimate case count numbers derived from these figures [15]. To ensure accuracy of extractions, monthly case count estimates were summed and compared with the reported annual national case counts. Incidence was estimated using U.S. national and state-level population denominators obtained from the U.S. Census Bureau [16]. Where necessary, estimates for inter-censal years were estimated via linear interpolation and extrapolation.

Environmental exposure data

As noted above, ENSO is a complex climatic phenomenon manifested by changes in sea-surface temperature and atmospheric pressure over the Pacific Ocean. ENSO has multiple attributes, including sea-surface temperature, wind, air temperature and cloud anomalies. For simplicity, we used the National Oceanic and Atmospheric Administration (NOAA) multivariable ENSO index (MEI) [17] as our measure of ENSO activity. The MEI is scaled from -3 (consistent with 'La Niña'-like conditions) to $+3$, with high values corresponding to ENSO events. Monthly MEI values for January 1999 to December 2014 were obtained from the NOAA [17].

Although the effects of ENSO on North American weather are widespread, the strongest effects are observed in western states, and to some extent on Gulf states. Weather and ocean temperatures on the east coast of the United States are influenced by the North Atlantic Oscillation (NAO) index [18], which manifests as fairly regular fluctuations in atmospheric pressure between Iceland and the Azores. The resultant pressure gradient influences land and sea-surface temperatures, and precipitation patterns, in North America and Europe. Our measure of NAO strength, which we also obtained from the NOAA, was the NAO Index.

Like the MEI, this index is scaled from -3 to $+3$, with higher values associated with warmer temperatures and increased precipitation in the eastern United States and lower values associated with cooler, dryer conditions [18]. Unlike ENSO, which is defined in part by sea-surface temperature anomalies, the relationship between sea-surface temperature and NAO appears to be more complex. While certain analyses suggest an inverse relationship between NAO and sea-surface temperatures at prolonged (4 year) lags [19], others suggest reversed causation, with NAO linked to preceding sea-surface temperature anomalies in the Gulf Stream [20].

Statistical analysis

National analyses

We evaluated year-on-year and seasonal trends in overall vibriosis incidence in the United States using count-based regression models that incorporated linear, quadratic and cubic multi-annual trends, as well as fast Fourier transforms to account for seasonal oscillation. As both deviance and Pearson's goodness-of-fit statistics suggested overdispersion of count data, negative binomial models were constructed. Census population estimates were used as model offsets with interpolation used to generate populations in inter-censal years.

Initial estimates of the lagged impact of ENSO and NAO on disease risk were generated by incorporating monthly MEI and NAO index values into trend models at lags of 1–12 months. Models were constructed by backward elimination, with covariates retained for $P < 0.2$. Combined incidence rate ratios (IRRs) and standard errors for ENSO and NAO exposures at multiple lags were generated via linear combination [21].

The inclusion of multiple-lagged exposures can result in several challenges, including difficulties with model interpretation, correlation in exposures at multiple lags and non-parsimony of models. We therefore constructed distributed lag non-linear models to evaluate the integrated effects of environmental exposures at multiple lags [22]. These models characterise exposures as two-dimensional risk planes, referred to as 'cross-bases', and are defined as level of exposure by lag. We created two cross-bases, for MEI and NAO, at values ranging from -3 to $+3$, across 12 month lags, which were incorporated into generalised linear models that also adjusted for seasonality, and linear and cubic trends, using a log-link function, in order to approximate negative binomial models constructed above. We assumed that ENSO and NAO effects on risk would be linear at any given lag, but modelled lag structure as a cubic polynomial. Both ENSO and NAO effects were evaluated at the uppermost extreme ($+3$) value, with index values of zero serving as referents.

Regional analyses

COVIS reports annual vibriosis counts by state, with states grouped together according to the nature of their coastlines (Pacific, Gulf, Atlantic or non-coastal). We evaluated relative incidence in each grouping using negative binomial models with state populations used as model offsets. We also evaluated linear trend terms from 1999 to 2014 for each region, and the associations between vibriosis risk and annual mean ENSO and NAO values. The non-coastal region was used as a referent. Regional differences in trend terms, and the effect of average annual ENSO and NAO values, were evaluated using the Cochrane's Q-statistic, with inverse variance weighting [23].

Table 1. Temporal trends and impact of environmental exposures on national vibriosis incidence

	Temporal trend model			Temporal trend model with environmental exposures		
	IRR ^a	95% CI		IRR ^a	95% CI	
Year	1.071	1.061	1.081	1.074	1.064	1.084
Sine (month)	0.453	0.427	0.481	0.449	0.423	0.477
Cosine (month)	0.401	0.377	0.426	0.407	0.384	0.433
MEI						
3-month lag	-	-	-	1.122	1.051	1.197
5-month lag	-	-	-	0.939	0.875	1.007
10-month lag	-	-	-	1.088	1.026	1.153
Linear combination of MEI coefficients	-	-	-	1.145	1.065	1.232
NAO						
3-month lag	-	-	-	1.034	0.995	1.075
5-month lag	-	-	-	0.967	0.929	1.007
10-month lag	-	-	-	1.031	0.987	1.077
11-month lag	-	-	-	1.029	0.986	1.074
12-month lag	-	-	-	0.970	0.931	1.010
Linear combination of NAO coefficients	-	-	-	1.064	0.983	1.151

MEI, multivariable ENSO index; NAO, North Atlantic Oscillation index.

^aPer 1-point increase in monthly MEI or NAO.

Linear trends in risk for each state were generated by estimating the year-on-year IRR for vibriosis by state. Negative binomial models for six states (Colorado, Iowa, Nebraska, New Mexico, South Carolina and West Virginia) failed to converge. To evaluate whether trends might exhibit a north-south gradient suggestive of climate change effects, we constructed meta-regressive models using the latitude of state centroids as the explanatory variable [24]. Our hypothesis was that relative rate of increase in risk due to climate change would be greater at northern than southern latitudes, particularly in coastal states, due to ocean warming.

All data used in this study are pre-collected aggregate counts and are publicly available. Negative binomial models and meta-regression models were constructed using Stata Intercooled version 15 (Stata Corp., College Station, Texas), while distributed lag non-linear models were constructed using the *dlm* package for R, version 3.1.5 [25]. Datasets used for analyses can be obtained via Figshare at https://figshare.com/articles/Vibriosis_data_files/6856427.

Results

From 1999 to 2014, a total of 10 800 cases of vibriosis were contained in COVIS reports, with an additional 62 cases noted as part of a *V. parahaemolyticus* outbreak in Alaska in 2004. Of these 10 862 cases, we were able to assign 10 102 (93.0%) to a month of year in national-level data, while 10 857 (>99.9%) could be assigned to a specific state. Crude national incidence increased threefold during the period under observation, from 0.11 cases per 100 000 population in 1999 to 0.36 cases per 100 000 population in 2014, representing a 7% average annual increase in incidence (IRR 1.071, 95% confidence interval (CI) 1.061–1.081). Significant seasonal oscillation was observed ($P < 0.001$) with a

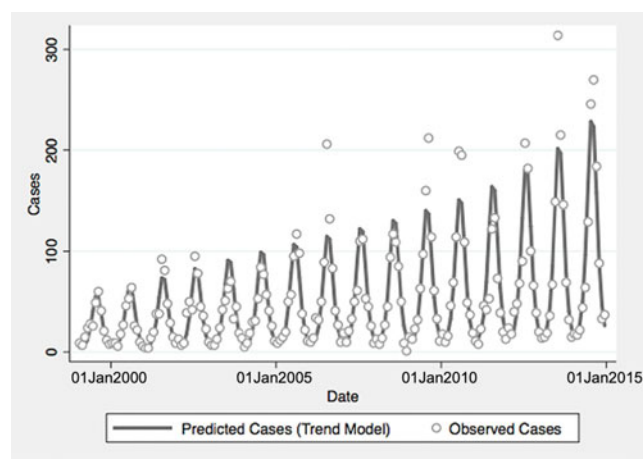


Fig. 1. Reported and model-predicted monthly vibriosis counts, United States 1999–2014. Observed counts are represented by circles; solid curve represents predictions from negative binomial model incorporating fast Fourier transform and year terms. Date is plotted on the X-axis; counts are plotted on the Y-axis.

summertime predominance. As quadratic trend terms were not significantly associated with risk, and cubic trend terms were associated with a worsening of Akaike's information criterion, the final trend model included only a linear term for year, as well as a fast Fourier transform (Table 1).

ENSO was associated with enhanced risk of vibriosis at 3 and 10 month lags while ENSO at a 5 month lag was associated with attenuated risk. The overall effect of combined ENSO coefficients significantly increased vibriosis risk (combined IRR 1.145, 95% CI 1.064–1.231, $P < 0.001$). NAO effects were retained in the model

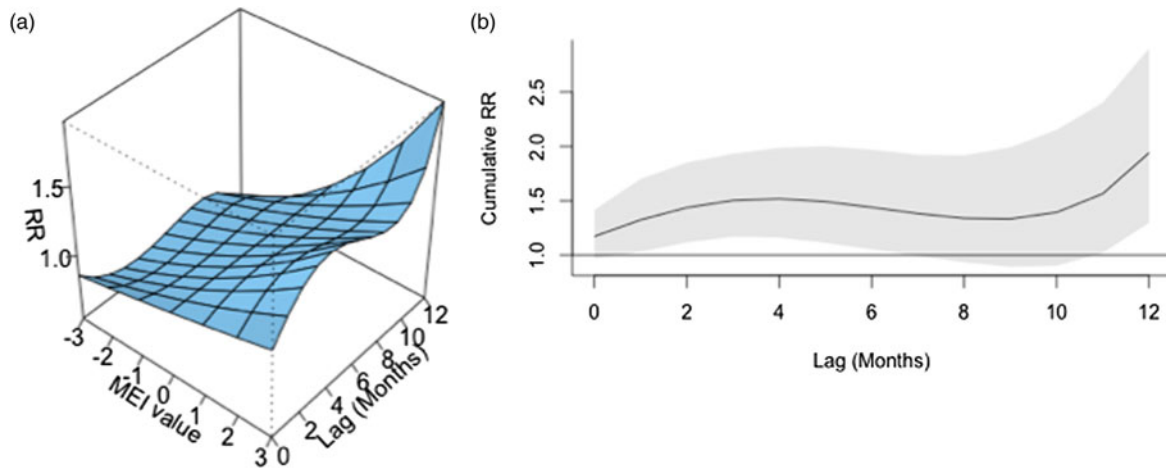


Fig. 2. Association between lagged MEI and vibriosis risk, United States 1999–2014. (a) Risk surface represents modelled association between the MEI (scaled from -3 , most La Niña-like, to $+3$, most El Niño-like, X-axis) and monthly vibriosis risk over 1–12 month lags (Y-axis). Associated RRs are plotted on the Z-axis. (b) Cross-sectional RR associated with the MEI of $+3$; lagged El Niño-like conditions are associated with downstream integrated RR of vibriosis (RR 1.940, 95% CI 1.298–2.900).

Table 2. Temporal trends, regional differences and impact of environmental exposures on annual vibriosis incidence in states

	IRR ^a	95% CI	
Year	1.108	1.090	1.126
Yearly average MEI	1.169	1.012	1.350
Yearly average NAO	0.909	0.758	1.091
Region			
Non-coastal	1.000	(Referent)	
Atlantic	4.125	3.491	4.873
Pacific	13.412	10.607	16.960
Gulf	7.752	6.167	9.744

MEI, multivariable ENSO index; NAO, North Atlantic Oscillation index.

^aPer 1-point increase in yearly average MEI or NAO.

at five different lags (3, 5 and 10–12 months), and were inconsistent in effect. Overall, the combined effect of NAO was non-significant (IRR 1.064, 95% CI 0.983–1.151, $P=0.12$) (Table 1, Fig. 1). Distributed lag non-linear models of ENSO effect were also associated with a significant increase in vibriosis across lags of 1–12 months (integrated IRR 1.940, 95% CI 1.298–2.901). The integrated effect of NAO was again non-significant in distributed lag models (IRR 0.988, 95% CI 0.607–1.607) (Fig. 2).

As expected, regional analyses identified highest risks of infection in the Pacific (IRR 13.412, 95% CI 10.607–16.959) and Gulf (IRR 7.752, 95% CI 6.167–9.744) regions, with elevated risk in the Atlantic region (IRR 4.125, 95% CI 3.491–4.873). Overall, yearly average ENSO was associated with a significant increase in vibriosis risk (IRR per 1 unit increase in mean MEI 1.169, 95% CI 1.012–1.350), while yearly average NAO was not associated with increased risk (Table 2).

Significant increases in vibriosis risk were observed in non-Pacific regions during the period under observation, with significant heterogeneity in rate of change across regions (P for heterogeneity <0.001); in the Pacific region, a non-significant increasing trend was observed ($P=0.067$). The most marked

Table 3. Regional models of annual vibriosis incidence

	IRR ^a	95% CI	
Atlantic			
Year	1.117	1.108	1.127
Yearly mean MEI	1.032	0.959	1.111
Yearly mean NAO	0.838	0.774	0.907
Pacific			
Year	1.051	0.997	1.108
Yearly mean MEI	1.601	1.031	2.486
Yearly mean NAO	1.267	0.727	2.209
Gulf			
Year	1.050	1.042	1.058
Yearly mean MEI	1.016	0.948	1.089
Yearly mean NAO	1.031	0.947	1.123
Non-coastal			
Year	1.127	1.096	1.159
Yearly mean MEI	1.174	0.916	1.505
Yearly mean NAO	0.873	0.642	1.188

MEI, multivariable ENSO index; NAO, North Atlantic Oscillation index.

^aPer 1-point increase in yearly average MEI or NAO.

increases in vibriosis risk were detected in the Atlantic and non-coastal regions (i.e. regions with the lowest incidence at baseline). In regional models, a 1 unit increase in mean MEI was associated with a 60% increase in vibriosis risk in the Pacific region, but no significant effect of ENSO on risk was observed in other regions. No significant change in risk was observed with NAO in any region. Neither ENSO nor NAO effects were associated with significant regional heterogeneity (P for heterogeneity = 0.50 for ENSO; $P=0.52$ for NAO) (Table 3 and Fig. 3).

State-level IRRs were also markedly heterogeneous ($P < 0.001$). In meta-regression models, increasing latitude was associated with the relative magnitude of increased relative risk (RR per 10°

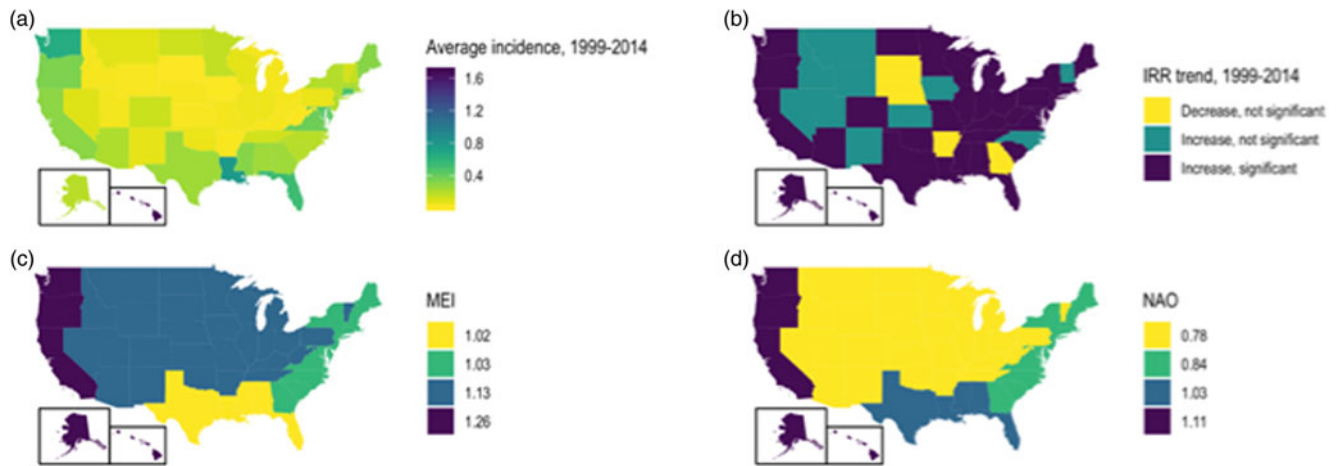


Fig. 3. State-level incidence, trends and environmental influence on annual vibriosis risk in the U.S. states, 1999–2014. (a) Mean annual vibriosis incidence per 100 000 population, by state; (b) IRRs for year-on-year change in vibriosis incidence from negative binomial models, by state; (c) trends in vibriosis incidence from negative binomial models, by state; (d) IRR for vibriosis risk with a 1-unit change in the MEI, by region. Six grey-shaded states are those for which negative binomial models failed to converge.

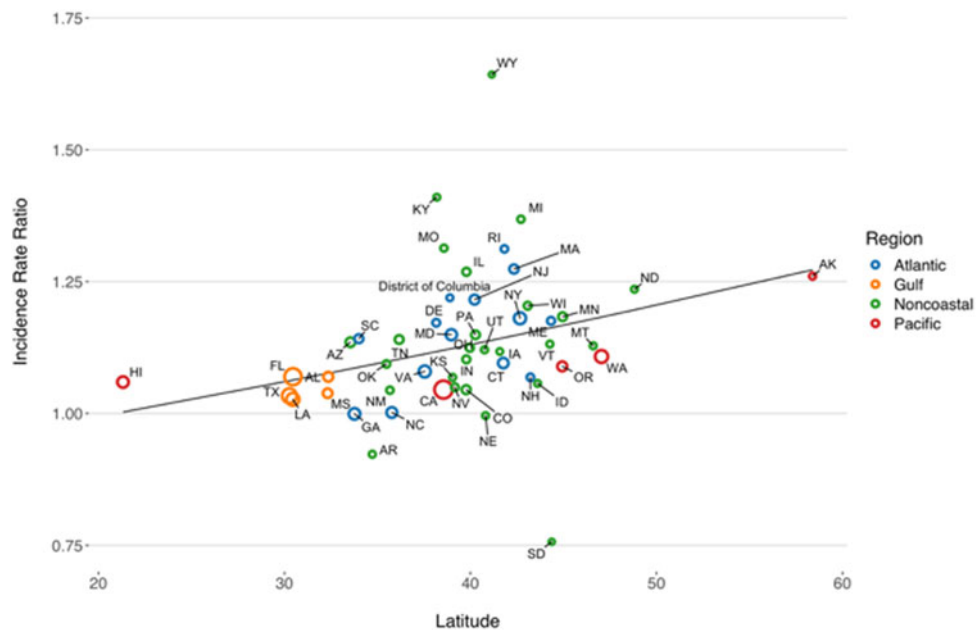


Fig. 4. Association between latitude and linear trend in vibriosis incidence, United States 1999–2014. Correlation between state latitude and average yearly IRR for vibriosis. Each circle represents a single U.S. state or District of Columbia, with size inversely proportional to variance in IRR estimates, corresponding to the weight assigned to each state. Circles are colour coded according to COVIS regions. Fitted lines represent the association between state latitude and IRR as predicted using univariable meta-regression (relative change in IRR per 10° increase in latitude of state centroid 1.059, 95% CI 1.020–1.099). Note that six states for which negative binomial models did not converge are excluded.

increase in latitude of state centroid 1.059, 95% CI 1.020–1.099). Adjustment for latitude resulted in a 36% reduction in between-study variance (τ^2) [26]. There was no significant association between region and rate of change, after adjustment for latitude. We also found no significant interaction between latitude and whether or not a state was coastal (P for multiplicative interaction term = 0.87) (Fig. 4).

Discussion

Given that toxigenic *V. cholerae* is a sentinel global pathogen due to its virulence, capacity for genetic reassortment and epidemic

potential, the ecology and dynamics of this pathogen have been extensively studied [10, 27, 28]. However, other *Vibrio* species of public health importance can also cause severe human disease, and their associated disease burden appears to be increasing. An increase in disease incidence may reflect increased pathogen abundance in salt-water environments, as well as an increase in the prevalence of immune compromised states in the human population, as individuals with immune compromise or iron overload states appear to be at greatest risk for severe vibriosis [3]. Due to the thermophilic nature of *Vibrio* species and their increased abundance in warmer waters with decreased salinity, there is reason to anticipate that *Vibrio* infection incidence will

increase in coming decades as a result of climate change-associated ocean warming [12].

Using publicly available *Vibrios* case count data from the United States COVIS system, we evaluated vibriosis trends and their relation with large-scale oceanic phenomena. We also examined the association between rate of increase and latitude, as we hypothesised that relative increases in risk would be greatest at northernmost latitudes where vibriosis has historically been less common. Our observations suggest that climate change-driven range expansion may be in progress for this disease, and the sensitivity of vibriosis incidence to El Niño-like conditions suggests that climate change is likely to drive further increases in vibriosis incidence in the future. After adjusting for long-term trends and seasonal oscillation, we found vibriosis incidence in the United States to be very sensitive to the ENSO. Using distributed lag non-linear models to examine risk effects at multiple lags, we found that vibriosis incidence in the United States is expected to double in the year after strong ENSO-like conditions (MEI = 3). This finding is consistent with existing work on the ecology of cholera in low- and middle-income countries [9, 29]. The regional analyses suggested these effects are concentrated in the Pacific region, where states are most strongly teleconnected to ENSO and where baseline vibriosis incidence is the highest.

Strong ENSO effects may provide insight into future changes in disease epidemiology that may occur under climate change scenarios such as increases in temperature, precipitation anomalies and ocean warming effects [11]. As current anthropogenic climate change is a global phenomenon with no recent precedent, it has been noted that the irregular nature of ENSO allows it to serve as a natural experiment for exploring future climate change effects [11]. The mechanisms whereby ENSO might increase vibriosis risk are likely to be complex; however, conditions like changes in salinity, ocean warming and increased abundance of nutrients and flow of freshwater into oceans are all associated with ENSO [30, 31], as well as with *Vibrio* abundance [32, 33]. It should be noted that, as with *V. cholerae*, NCV have complex ecology, and their abundance may be impacted by the abundance of the cyanobacteria and dinoflagellates with which they are associated; these microbial populations are also sensitive to changes in nutrients, water temperature and salinity such as those that accompany ENSO [31, 34]. The complexity of *Vibrio* ecology, shown by differing effects of ENSO at multiple lags due to its impact on different components of the ecosystem, make the distributed lag approach we have applied particularly attractive.

Since weather and sea-surface warming in the Pacific region are more likely to be influenced by ENSO than the Atlantic region of the United States, we also explored the impact of the NAO on vibriosis incidence. We hypothesised that NAO would be associated with regional vibriosis incidence in the Atlantic and possibly the Gulf regions. However, compared with the large effects observed with ENSO at the national level and in the Pacific region, the effects associated with NAO were inconsistent in national analyses, and absent in regional analyses. Given that NAO is predominantly a pressure phenomenon (rather than a phenomenon explicitly related to ocean temperature like ENSO), the absence of clear and consistent links to vibriosis may be unsurprising.

Range expansion of vibriosis has been reported in Northern Europe and appears to correlate with increasing Baltic-Sea temperatures [12]. We therefore sought to evaluate the possibility that there was a north-south gradient in rate of change in vibriosis risk in the United States. The meta-regression approach we

applied here was identical to the approach applied in our earlier work on Lyme disease [24]. The gradient we observed would be consistent with range expansion for vibriosis risk as a result of warmer oceans at higher latitudes. However, other mechanisms (such as increased reporting in jurisdictions not previously believed to be risk-areas for vibriosis) could produce similar patterns. This is possible since the COVIS system has observed increased coverage and increased case submission over time, particularly once NCV became nationally notifiable in 2007 [6]. However, given that similar trends in rates of vibriosis have been reported using FoodNet data, which involve active rather than passive surveillance, it is unlikely that these trends reflect a reporting artefact [3].

Furthermore, an ocean warming effect would be consistent with the ENSO effects observed nationally, and in the Pacific region, in our initial analyses. Indeed, the substantial face-validity of the ENSO effects we observe supports the use of this irregular climatic phenomenon as a 'natural experiment' that can be used to anticipate impacts of future climatic change on infectious diseases caused by pathogens with environmental reservoirs. Given the unprecedented and global nature of anthropogenic climate change, evaluation of effects in a 'control' population or control period is not possible [35]. While year-on-year increases in disease incidence could be attributable to gradual increase in land and sea-surface temperatures, it is difficult to attribute such changes to climate as opposed to other time-varying effects, such as changing characteristics of diagnostic tests or surveillance systems [36]. In this context, creative use of irregular ecological exposure data may provide insights into climate-driven disease risk that inform policy and prevention efforts.

Our analysis is inevitably subject to limitations. As we only have access to case counts by time period and region, we cannot account for changing reporting behaviour as a driver for observed trends. However, it should be noted that we do account for such temporal trends in our models, and the ENSO effects we observe are robust after accounting for trends, regardless of their underlying mechanism. Our lack of access to individual case data means that we cannot perform nuanced subgroup analyses that consider case comorbidity or exposure history. Extracting case counts from graphical plots produced counts similar to those contained in reports, but is likely to have resulted in some random misclassification of these counts; while this may have resulted in diminished statistical power, such misclassification would not have resulted in spurious associations or systematic bias in effects. Similarly, non-differential misclassification of exposure, as may have occurred in regional analyses if we attributed illness to a particular state whereas exposure occurred in a different state, would have biased our results towards the null, making the (strong) effects we observe here lower bound estimates.

In summary, we used publicly available data on vibriosis incidence in the United States to perform the first (to our knowledge) evaluation of the possible contributions of ongoing environmental change to observed increases in vibriosis incidence in North America. Broadly, we found two lines of evidence suggesting that climatic change and ocean warming may be important drivers of observed increases in risk. First, *Vibrio* risk was strongly associated with lagged ENSO-like oceanic changes, and second, a north-south gradient in relative increase in risk. Attributing such changes to ocean warming and climatic change is biologically plausible, and consistent with effects observed in other geographic locales with *V. cholerae*. Our work suggests that vibriosis may be an important sentinel for infectious disease

impacts of climate change, and our methods also present a model that can be applied to other infectious diseases. Anticipating future trends in vibriosis as oceans warm may help with projections of likely future burden of disease, and may help guide and prioritise preventive strategies.

Conflict of interest. None of the authors has any conflict of interest, financial or otherwise, associated with this work.

References

1. **Armstrong G, Hollingsworth J and Morris J Jr.** (1998) Bacterial food-borne infections. In Evans A and Brachman P (eds), *Bacterial Infections of Humans: Epidemiology and Control*, 3rd Edn. New York: Plenum Medical Book Company, pp. 109–138.
2. **Franca SM et al.** (1980) *Vibrio parahaemolyticus* in Brazilian coastal waters. *JAMA* **244**, 587–588.
3. **Newton A et al.** (2012) Increasing rates of vibriosis in the United States, 1996–2010: review of surveillance data from 2 systems. *Clinical Infectious Diseases* **54**(Suppl 5), S391–S395.
4. **Mahon BE et al.** (1996) Reported cholera in the United States, 1992–1994: a reflection of global changes in cholera epidemiology. *JAMA* **276**, 307–312.
5. **Dechet AM et al.** (2008) Nonfoodborne *Vibrio* infections: an important cause of morbidity and mortality in the United States, 1997–2006. *Clinical Infectious Diseases* **46**, 970–976.
6. **Wong KC et al.** (2015) Antibiotic use for *Vibrio* infections: important insights from surveillance data. *BMC Infectious Diseases* **15**, 226.
7. **Martinez-Urtaza J et al.** (2013) Spread of Pacific Northwest *Vibrio parahaemolyticus* strain. *New England Journal of Medicine* **369**, 1573–1574.
8. **Semenza JC et al.** (2017) Environmental suitability of *Vibrio* infections in a warming climate: an early warning system. *Environmental Health Perspectives* **125**, 107004.
9. **Hashizume M et al.** (2011) The Indian Ocean dipole and cholera incidence in Bangladesh: a time-series analysis. *Environmental Health Perspectives* **119**, 239–244.
10. **Pascual M et al.** (2000) Cholera dynamics and El Niño-Southern Oscillation. *Science* **289**, 1766–1769.
11. **Fisman DN, Tuite AR and Brown KA** (2016) Impact of El Niño Southern Oscillation on infectious disease hospitalization risk in the United States. *Proceedings of the National Academy of Sciences USA* **113**, 14589–14594.
12. **Baker-Austin C et al.** (2013) Emerging *Vibrio* risk at high latitudes in response to ocean warming. *Nature Climate Change* **3**, 73–77.
13. **Heilpern KL and Borg K** (2006) Update on emerging infections: news from the Centers for Disease Control and Prevention. *Vibrio* illness after Hurricane Katrina – multiple states, August–September 2005. *Annals of Emergency Medicine* **47**, 255–258.
14. **National Center for Emerging and Zoonotic Infectious Diseases** (2016) *Cholera and Other Vibrio Illness Surveillance (COVIS)*. Atlanta, Georgia: U.S. Centers for Disease Control and Prevention. <https://www.cdc.gov/vibrio/surveillance.html>
15. **Rohatgi A** (2019) *WebPlotDigitizer*. San Francisco, CA: Automeris. Available at <https://auto.meris.io/WebPlotDigitizer/> (Last accessed 16 July 2018).
16. **U.S. Bureau of the Census, U.S. Department of Commerce** (2018) *State Population Totals and Components of Change: 2010–2017*. Washington, DC, USA: U.S. Department of Commerce. Available at <https://www.census.gov/data/tables/2017/demo/pepstat-total.html> (Last accessed 19 July 2018).
17. **Wolter K** (2018) *Multivariate ENSO Index (MEI)*. Washington, DC: National Oceanic and Atmospheric Administration. Available at <https://www.esrl.noaa.gov/psd/enso/mei/table.html> (Last accessed 19 July 2018).
18. **North Atlantic Oscillation (NAO)** (2018) *National Oceanic and Atmospheric Administration (NOAA)*. Washington, DC: National Oceanic and Atmospheric Administration. Available at <https://www.ncdc.noaa.gov/teleconnections/nao> (Last accessed 19 July 2018).
19. **Xu H et al.** (2015) Impacts of the North Atlantic Oscillation on sea surface temperature on the Northeast US Continental Shelf. *Continental Shelf Research* **105**, 60–66.
20. **Wang W et al.** (2004) The relation between the North Atlantic Oscillation and SSTs in the North Atlantic Basin. *Journal of Climate* **17**, 4752–4759.
21. **Hosmer D and Lemeshow S** (2000) Interpretation of the fitted logistic regression model. In Walter A. Shewhart and Samuel S. Wilks (eds), *Applied Logistic Regression*. New York: John Wiley and Sons, pp. 47–90.
22. **Gasparrini A, Armstrong B and Kenward MG** (2010) Distributed lag non-linear models. *Statistics in Medicine* **29**, 2224–2234.
23. **Serghiou S and Goodman SN** (2018) Random-effects meta-analysis: summarizing evidence with caveats. *JAMA* **321**, 301–302.
24. **Tuite AR, Greer AL and Fisman DN** (2013) Effect of latitude on the rate of change in incidence of Lyme disease in the United States. *CMAJ Open* **1**, E43–E47.
25. **R Core Team** (2018) *R: A Language and Environment for Statistical Computing*. Vienna, Austria: Foundation for Statistical Computing. Available via the Internet at <https://www.R-project.org/> (Last accessed 19 July 2018).
26. **Abubakar I et al.** (2013) Systematic review and meta-analysis of the current evidence on the duration of protection by bacillus Calmette-Guérin vaccination against tuberculosis. *Health Technology Assessment* **17**, 1–372, v–vi.
27. **Lipp EK, Huq A and Colwell RR** (2002) Effects of global climate on infectious disease: the cholera model. *Clinical Microbiology Reviews* **15**, 757–770.
28. **Gil AI et al.** (2004) Occurrence and distribution of *Vibrio cholerae* in the coastal environment of Peru. *Environmental Microbiology* **6**, 699–706.
29. **Alajo SO, Nakavuma J and Erume J** (2006) Cholera in endemic districts in Uganda during El Niño rains: 2002–2003. *African Health Sciences* **6**, 93–97.
30. **Hasegawa T, Ueki I and Ando K** (2017) El Niño–Southern Oscillation-time scale covariation of sea surface salinity and freshwater flux in the western tropical and northern subtropical Pacific. *Geophysical Research Letters* **44**, 6895–6903.
31. **Chavez FP et al.** (1999) Biological and chemical response of the equatorial Pacific Ocean to the 1997–98 El Niño. *Science* **286**, 2126–2131.
32. **Constantin de Magny G et al.** (2008) Environmental signatures associated with cholera epidemics. *Proceedings of the National Academy of Sciences USA* **105**, 17676–17681.
33. **Raszl SM et al.** (2016) *Vibrio parahaemolyticus* and *Vibrio vulnificus* in South America: water, seafood and human infections. *Journal of Applied Microbiology* **121**, 1201–1222.
34. **Morales-Ramirez A and Brugnoli-Olivera E** (2001) El Niño 1997–1998 impact on the plankton dynamics in the Gulf of Nicoya, Pacific coast of Costa Rica. *Revista de Biología Tropical* **49**(Suppl 2), 103–114.
35. **Hsiang SM, Meng KC and Cane MA** (2011) Civil conflicts are associated with the global climate. *Nature* **476**, 438–441.
36. **Kontopantelis E et al.** (2015) Regression based quasi-experimental approach when randomisation is not an option: interrupted time series analysis. *BMJ* **350**, h2750.